ACS OMEGA

http://pubs.acs.org/journal/acsodf

Article

Stereospecific Formation of the *rctt* Isomer of Bis-crown-Containing Cyclobutane upon [2 + 2] Photocycloaddition of an (18-Crown-6)stilbene Induced by Self-Assembly via Hydrogen Bonding

Timofey P. Martyanov,* Artem P. Vorozhtsov, Nadezhda A. Aleksandrova, Ilia V. Sulimenkov, Evgeny N. Ushakov, and Sergey P. Gromov*

Cite This: *ACS Omega* 2022, 7, 42370−42376

Read Online

ACCESS | Metrics & More | Article Recommendations | Supporting Information

ABSTRACT: The formation and the spectroscopic and structural properties of 1:1 and 2:1 (ligand-to-dication) complexes of an (18-crown-6)stilbene with ethane-1,2-diammonium diperchlorate in MeCN were studied by UV−vis and NMR spectroscopy and by density functional theory calculations. Prolonged UV irradiation of 2:1 mixtures of the crown stilbene and the diammonium salt led to the formation of two main photoproducts, namely, the single *syn*-"head-to-head" photodimer of the crown stilbene (*rctt* cyclobutane) due to supramolecular-assisted [2 + 2] photocycloaddition and a crown ether derivative of phenanthrene due to a photoinduced electrocyclization reaction. The *rctt* cyclobutane was isolated by preparative photolysis, followed by chromatography. The selectivity of the [2 + 2] photocycloaddition is explained by supramolecular pre-organization of crown stilbene molecules into the 2:1 complexes that have a pseudo-sandwich structure with stacking interactions between the stilbene moieties.

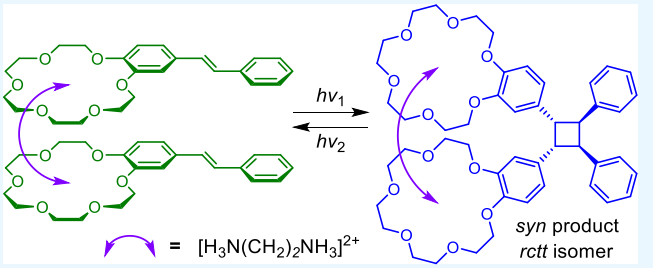

INTRODUCTION

Photocycloaddition (PCA) reaction of unsaturated compounds resulting in cyclobutane derivatives is widely used in organic[1−5] and materials chemistry.[6,7] The synthesis of 1,2,3,4-tetraarylcyclobutanes in solutions is complicated by short lifetimes of the electronically excited states of the starting reactants (diarylethylenes).[8] This problem and also the problem of low stereospecificity of PCA can be solved by means of supramolecular pre-organization of olefin molecules.[8−10] As a rule, diarylethylenes are assembled to dimers and heterodimers using metal cations[11] or supramolecular containers[12−15] such as cucurbiturils and cyclodextrins. We are developing a different approach, that is, self-assembly through hydrogen bonding.[16−18] Previously, we showed[19−21] that in the presence of diammonium cations in solutions, bis(18-crown-6)stilbene (**BCS**) forms 2:2 complexes. Owing to the ditopic coordination, the PCA reaction in these complexes proceeds stereoselectively in a high quantum yield. In this study, we verified whether the two-site complexation in bisligand complexes of crown-containing stilbene is necessary for effective PCA reaction. As investigation objects, we used the monocrown ether analogue, (18-crown-6)stilbene (*E*)-**S**, and its complexes with alkanediammonium ion $^{+}H_3N(CH_2)_2NH_3^{+}$ ($\mathbf{A}^{2+}$).

RESULTS AND DISCUSSION

Crown stilbene (*E*)-**S** was prepared by a previously reported procedure.[18] The complex formation of (*E*)-**S** with ethane-1,2-diammonium ($\mathbf{A}^{2+}$) diperchlorate was studied by NMR titration in MeCN-d_3. Two equilibria may take place upon the addition of a diammonium salt to a solution of stilbene (*E*)-**S** (Scheme 1).

The complexation of stilbene (*E*)-**S** with $\mathbf{A}^{2+}$ induces downfield shifts of all aromatic and ethylene proton signals in the ^{1}H NMR spectrum (Figure 1). The greatest shift of almost 0.12 ppm was observed for 2,5,6-H protons. Considerable changes are also found in the aliphatic proton region (Figure S1b). The 3(4)-C*H*$_2$CH$_2$OAr signals shift downfield by 0.15 ppm during the titration. The behavior of the signals of 3(4)-CH$_2$OAr differs from the behavior of other signals; the direction of their displacement changes during the titration: they shift upfield in the beginning of the titration and shift downfield when excess $\mathbf{A}^{2+}$ is present. The upfield shift of the 3(4)-CH$_2$OAr signal of crown stilbene (*E*)-**S** observed in the deficiency of $\mathbf{A}^{2+}$ ($C_A/C_S \approx 0.5$, Figure S1b) attests to the

Received: August 25, 2022
Accepted: October 25, 2022
Published: November 8, 2022

https://doi.org/10.1021/acsomega.2c05295
ACS Omega 2022, 7, 42370−42376

Scheme 1. Complexation of (18-Crown-6)stilbene with the Ethanediammonium Ion

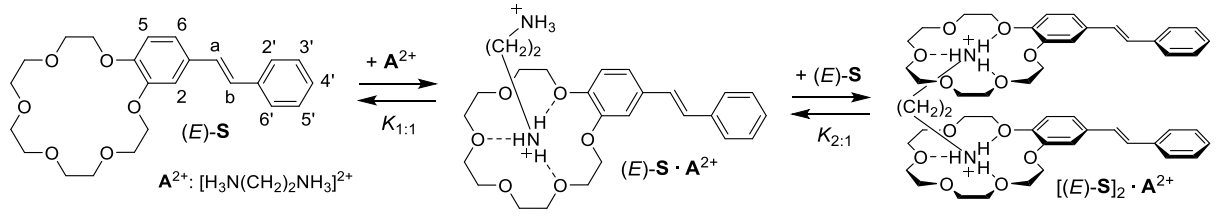

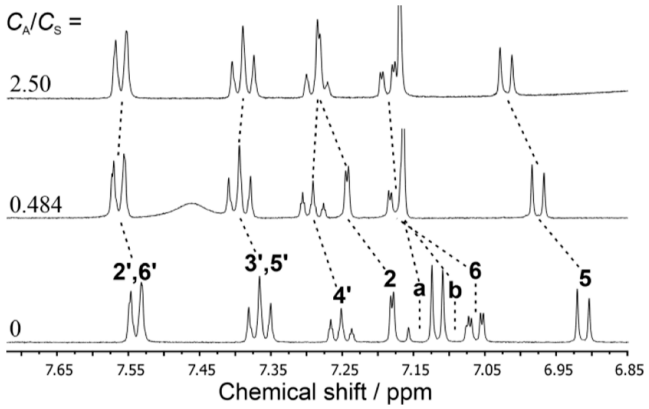

Figure 1. ^{1}H NMR spectra of stilbene (*E*)-**S** (C_S = 0.002 M) measured upon the addition of different amounts of $\mathbf{A}(ClO_4)_2$ (C_A) in MeCN-d_3.

formation of the bis-ligand complex in which the indicated atoms of one molecule are shielded by the other ligand molecule.

In the case of the **BCS** ligand, the formation of the 2:2 bispseudo-sandwich complex with the $\mathbf{A}^{2+}$ ions resulted in downfield shifts of the H-2,6 signals and upfield shifts of the H-5 signal and ethylene group signals (Figure S2). The latter unambiguously indicates the proximity of the two stilbene moieties in the $(\mathbf{BCS})_2{\cdot}(\mathbf{A}^{2+})_2$ complex. The fact that only downfield shifts are observed for the aromatic proton signals upon the formation of the $[(E)\text{-}\mathbf{S}]_2{\cdot}\mathbf{A}^{2+}$ complex suggests that the olefinic bonds in this complex are separated by a greater distance than those in $(\mathbf{BCS})_2{\cdot}(\mathbf{A}^{2+})_2$. One more explanation for this fact may be a higher population of unstacked conformers of $[(E)\text{-}\mathbf{S}]_2{\cdot}\mathbf{A}^{2+}$ compared to the stacked ones (Figure 5).

Using the results of NMR titration of stilbene (*E*)-**S** with ethanediammonium salt in MeCN-d_3 (Figure S3), the stability constants of complexes of various stoichiometries (Table 1)

Table 1. Stability Constants of the Complexes of Stilbene (*E*)-S with Ethanediammonium Ion A^{2+}[a]

complex	log*K*(NMR)	log*K*(SPT)
$(E)\text{-}\mathbf{S}{\cdot}\mathbf{A}^{2+}$	4.56	4.77
$[(E)\text{-}\mathbf{S}]_2{\cdot}\mathbf{A}^{2+}$	4.64	4.82

[a]In MeCN-d_3 or MeCN. The values were within about ±20%.

were calculated by the parameterized matrix modeling[22] according to the putative reaction model (Scheme 1). The formation of bisligand complexes is also supported by mass spectrometry data (Figure S4). Spectrophotometric titration (SPT) was additionally used to measure the stability constants. The addition of $\mathbf{A}(ClO_4)_2$ in MeCN to a solution of stilbene (*E*)-**S** resulted in a slight blue shift and an increase in intensity of the long-wavelength absorption band (Figures S8 and S9). The isosbestic points slightly changed the positions during the titration.

The stability constants determined by NMR for the (*E*)-**S**–$\mathbf{A}(ClO_4)_2$ system proved to be somewhat lower than the constants measured using the SPT data. This may be attributable to the larger amount of water in MeCN-d_3 compared to that in MeCN. The results (Table 1) attest to the enhanced stability of the bis-ligand complex $[(E)\text{-}\mathbf{S}]_2{\cdot}\mathbf{A}^{2+}$ relative to that of $(E)\text{-}\mathbf{S}{\cdot}\mathbf{A}^{2+}$, which may be due to additional intermolecular interactions in the case of stacking conformers.

After short-term (800 s) UV irradiation at λ = 313 nm of a MeCN solution of free stilbene (*E*)-**S**, an additional set of signals (*Z*-isomer) appears in the ^{1}H NMR spectrum of evaporated photolysate due to *E*–*Z* photoisomerization (Figures 2a,b and S11). After long-term (20 h) irradiation of

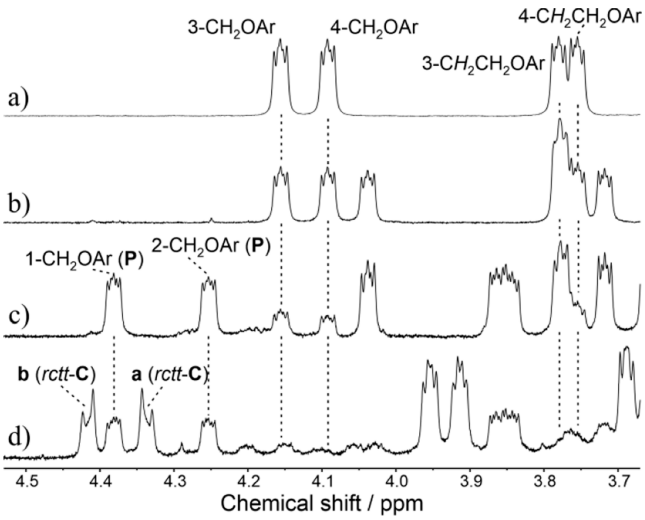

Figure 2. ^{1}H NMR spectra in DMSO-d_6 of free stilbene (*E*)-**S** (a), products of stilbene photolysis at 313 nm for 800 s (b) and for 20 h (c), products of photolysis of a 2:1 mixture of (*E*)-**S** and $\mathbf{A}(ClO_4)_2$ at 313 nm for 20 h (d). The photoirradiation was carried out for 0.001 M solutions of stilbene (*E*)-**S** (2 mL in a 1 cm cell) in MeCN located at equal distances from a mercury light.

a solution of (*E*)-**S** with the same light, the ^{1}H NMR spectrum of the photolysate exhibits new signals in the aromatic proton region at 7.4–8.8 ppm (Figure S12) and two multiplets shifted downfield relative to the crown ether proton signals (Figure 2c). Two singlets at 8.17 and 7.46 ppm are especially clearly defined. The only compound that could be characterized by this set of signals is phenanthrene derivative **P** (Scheme 2).[23] The formation of **P** is also confirmed by ESI-MS (Figure S6). In the ^{1}H NMR spectrum of photolysate formed from a (*E*)-**S** and $\mathbf{A}(ClO_4)_2$ mixture (2:1 molar ratio), apart from the proton signals of the above-indicated compounds, there are also two

https://doi.org/10.1021/acsomega.2c05295
ACS Omega 2022, 7, 42370–42376

Scheme 2. Formation of the Major Photoproducts upon Photolysis of a Pseudo-Sandwich Complex of (*E*)-S with the Ethanediammonium Ion A^{2+} in MeCN

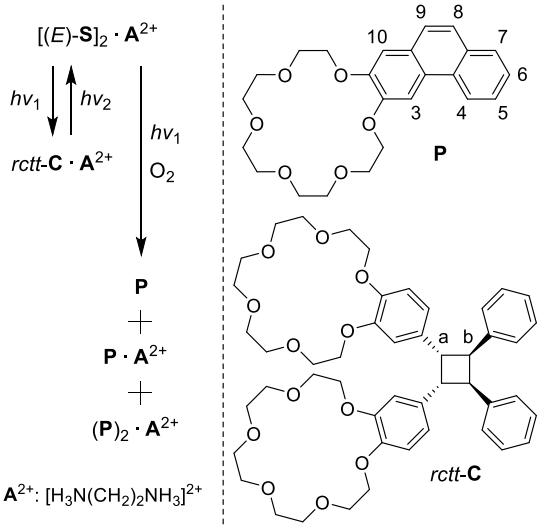

distorted doublets in the aliphatic region (4.42 and 4.34 ppm) with the vicinal ^3J constant of 7.2 Hz (Figures 2d and S15). These signals point to the formation of a cyclobutane ring with symmetrical positions of substituents. The aromatic region of the ^{1}H NMR spectrum also contained several new signals and two singlets at 10.02 and 9.82 ppm, which can be assigned to the aldehyde protons of benzaldehyde and 4′-formylbenzo-18-crown-6 ether, respectively. It is noteworthy that the observed signals of crown compounds in DMSO-d_6 correspond to free ligands since the stability of their complexes is much lower in DMSO than in MeCN.

The observed cyclobutane multiplets correspond to an AA′BB′ system. The PCA (photodimerization) reaction of olefins with two different substituents can give a total of 11 cyclobutane isomers.[8] Since $[(E)\text{-}\mathbf{S}]_2\cdot\mathbf{A}^{2+}$ is formed according to the head-to-head pattern, below we consider only the cyclobutane isomers **C** (Figure 3).

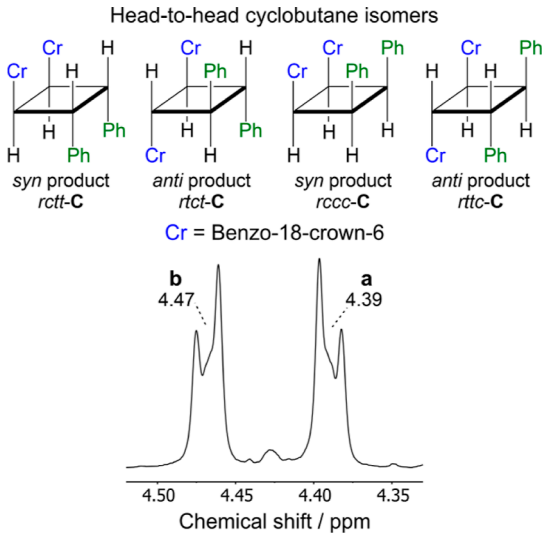

Figure 3. Probable head-to-head cyclobutane isomers **C** and fragment of the ^{1}H NMR spectrum of isolated *rctt*-**C** in MeCN-d_3.

The formation of isomers *rccc*-**C** and *rttc*-**C** from two *Z*-isomers of stilbene **S** is unlikely. The cause is the very short lifetime of the excited state of *Z*-stilbene.[24] Hence, PCA of complexes $[(E)\text{-}\mathbf{S}]_2\cdot\mathbf{A}^{2+}$ affords either cyclobutane *rctt*-**C** (*syn* adduct) or cyclobutane *rtct*-**C** (*anti* adduct). Previously,[11] the PCA reactions of sandwich complexes of (15-crown-5)-styrylpyridine with Ba^{2+} ions were shown to give a symmetrical *rctt* isomer of cyclobutane, manifested as two doublets of a similar shape at 4.53 and 4.40 ppm with ^3J = 6.4 Hz. It was shown[19] that the product of $(\mathbf{BCS})_2\cdot(\mathbf{A}^{2+})_2$ photolysis contained *rctt* and *rtct* cyclobutane isomers, with the former predominating. The cyclobutane ring protons in the *rtct* isomer (singlet at δ 3.40) appear in a higher field than those of the *rctt* isomer (singlet at δ 4.26). Thus, photolysis of a mixture of (*E*)-**S** with $\mathbf{A}(ClO_4)_2$ (Figure S15) gives cyclobutane *rctt*-**C** (50%), phenanthrene **P** (37%), benzaldehyde (7%), and 4′-formylbenzo-18-crown-6 ether (6%).

Oxygen removal from a mixture of (*E*)-**S** with $\mathbf{A}(ClO_4)_2$ by bubbling argon for 15 min had almost no effect on the percentage of phenanthrene **P** in the photolysate, but led to a decrease in percentage of aldehydes and, accordingly, to an increase in the percentage of cyclobutane *rctt*-**C** (Figure S16). Preparative photolysis in the presence of argon produced a sufficient amount of *rctt*-**C** for characterization (Figures 3 and S17).

A photochemical investigation was carried out to evaluate the efficiency of PCA. The irradiation of a 2:1 mixture of stilbene (*E*)-**S** and diammonium ($\mathbf{A}^{2+}$) salt at λ = 313 nm induced a decrease in the intensity of the long-wavelength absorption band of stilbene (*E*)-**S**, with the absorption maximum being shifted to shorter wavelengths (Figure 4). In

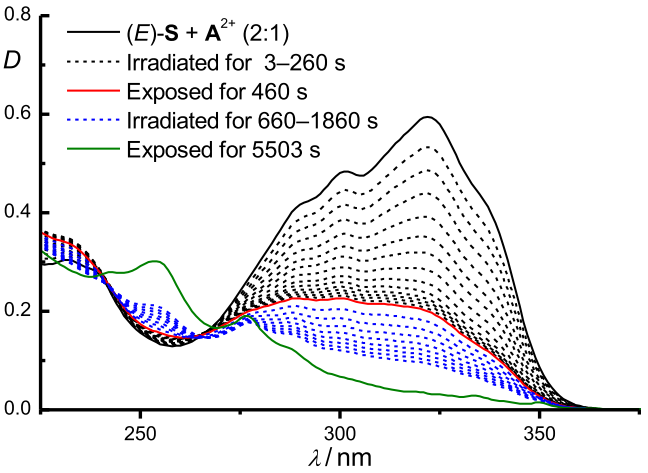

Figure 4. Steady-state photolysis data for a mixture of (*E*)-**S** and $\mathbf{A}(ClO_4)_2$ with λ = 313 nm light in MeCN (0.2 cm cell; the (*E*)-**S** concentration is 1×10^{-4} M and the $\mathbf{A}^{2+}$ concentration is 5×10^{-5} M).

the case of short irradiation times, the spectral changes corresponded to *E*−*Z* photoisomerization of stilbene derivatives.[18] Longer irradiation induced the formation of several new bands with peaks at 255, 277, 319, 334, and 350 nm. The 277 nm band referred to the cyclobutane *rctt*-**C**·$\mathbf{A}^{2+}$ complex, while the other bands apparently correspond to the formation of phenanthrene **P** and its complexes with $\mathbf{A}^{2+}$.

Using kinetic data of the steady-state photolysis (Figure 4), the effective quantum yields of electrocyclization Φ_{EL} (4.2×10^{-3}) and PCA Φ_{PCA} (5.7×10^{-3}) reactions were found.

https://doi.org/10.1021/acsomega.2c05295
ACS Omega 2022, 7, 42370−42376

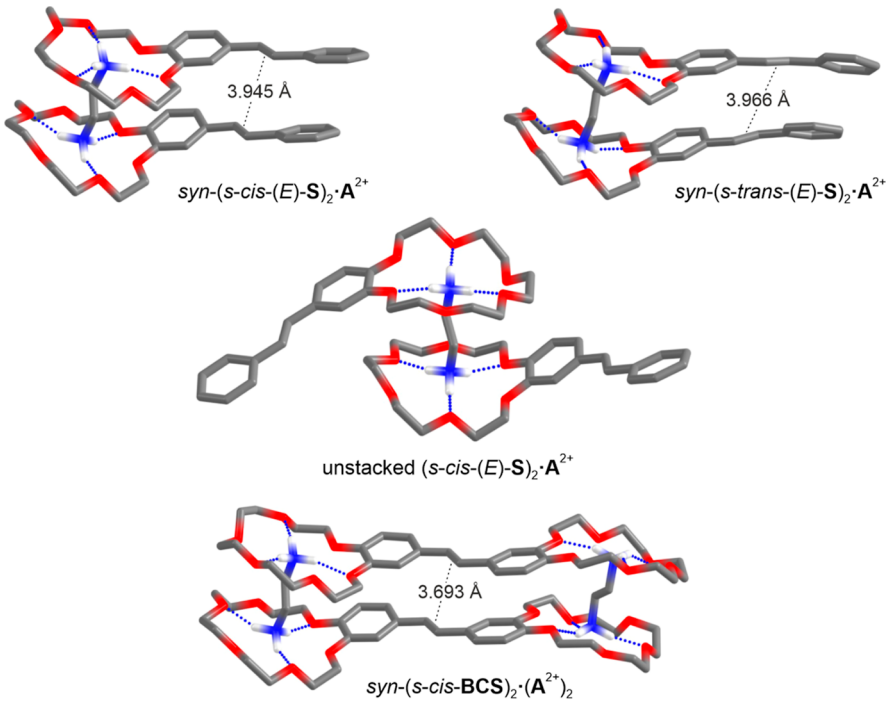

Figure 5. DFT-calculated geometries of selected stacked and unstacked conformers of complex $[(E)\text{-}\mathbf{S}]_2{\cdot}\mathbf{A}^{2+}$ and the low-energy *syn* conformer of complex $(\mathbf{BCS})_2{\cdot}(\mathbf{A}^{2+})_2$; hydrogen atoms are not shown except those of the ammonium groups.

Previously, we estimated the quantum yield of PCA for the 2:2 complex of **BCS** with $\mathbf{A}^{2+}$.[21] Owing to the two-site coordination, the PCA in $(\mathbf{BCS})_2{\cdot}(\mathbf{A}^{2+})_2$ had a high quantum efficiency of 0.27, which was almost 50 times higher than Φ_{PCA} for $[(E)\text{-}\mathbf{S}]_2{\cdot}\mathbf{A}^{2+}$. The most likely key reason for these differences is the minor amount of $[(E)\text{-}\mathbf{S}]_2{\cdot}\mathbf{A}^{2+}$ conformers that meet the topochemical requirements for the PCA reaction.[25] Also, some role can be played by the absence of alkoxyl substituents in the benzene ring of (*E*)-**S** in comparison with that of **BCS**, which is expected to disrupt the stacking interactions between the aromatic moieties of the ligands in the pseudo-sandwich complexes.[26] For isolated cyclobutane *rctt*-**C**, it was shown that irradiation at λ = 254 nm induced the retro-PCA reaction (Figure S23).

We performed a conformational analysis for complex $[(E)\text{-}\mathbf{S}]_2{\cdot}\mathbf{A}^{2+}$ in MeCN using DFT calculations (Figure S24, Table S1). Figure 5 shows two low-energy stacked conformers of $[(E)\text{-}\mathbf{S}]_2{\cdot}\mathbf{A}^{2+}$ with the *syn* orientation of the olefinic bonds relative to each other. These structures differ in the conformations of (*E*)-**S** (*s-trans* and *s-cis*) associated with rotation around the single bond between the benzocrown moiety and the olefinic bond. They are very close in the Gibbs free energy in solution (G_{soln}); the difference was calculated to be as low as 0.09 kcal mol^{-1} in favor of the *syn*-(*s-trans*)$_2$ conformer. The low-energy unstacked conformer of complex $[(E)\text{-}\mathbf{S}]_2{\cdot}\mathbf{A}^{2+}$ (Figure 5) was found to be more stable than the stacked *syn*-(*s-trans*)$_2$ conformer; the difference in G_{soln} was calculated to be 1.59 kcal mol^{-1}. This suggests the coexistence of the stacked and unstacked conformers in MeCN, the population of the former being relatively low. It should be noted that it is almost impossible to reliably estimate the relative populations of different conformers since a large number of low-frequency vibrational modes in these structures leads to a low accuracy in calculating the thermal correction to the Gibbs free energy.

Figure 5 also shows the low-energy *syn* conformer of complex $(\mathbf{BCS})_2{\cdot}(\mathbf{A}^{2+})_2$, whose stacked structure is predetermined by two-site coordination. The olefinic bonds in this conformer are almost parallel to each other (the angle between them is 0.76°) and are separated by a distance of 3.69 Å. This structure meets rather well the topochemical criteria for the PCA reaction. In contrast, the geometric parameters of the stacked *syn* conformers of complex $[(E)\text{-}\mathbf{S}]_2{\cdot}\mathbf{A}^{2+}$ are less suitable as regards the PCA reaction: the distances between the olefinic bonds in these conformers are larger by 0.25−0.27 Å than that in complex $(\mathbf{BCS})_2{\cdot}(\mathbf{A}^{2+})_2$, the angles between these bonds being also larger (6.05° for *syn*-(*s-cis*-(*E*)-**S**)$_2{\cdot}\mathbf{A}^{2+}$ and 16.49° for *syn*-(*s-trans*-(*E*)-**S**)$_2{\cdot}\mathbf{A}^{2+}$). The results of DFT calculations correlate with the experimental data obtained for complex $[(E)\text{-}\mathbf{S}]_2{\cdot}\mathbf{A}^{2+}$: both the lack of aromatic proton shielding (Figure 1) and the low efficiency of PCA (Φ_{PCA} = 5.7 × 10^{-3}) can be explained by two factors, first, a smaller population of stacked conformers of $[(E)\text{-}\mathbf{S}]_2{\cdot}\mathbf{A}^{2+}$ compared to unstacked ones and, second, a long distance between the olefinic bonds in the stacked conformers.

CONCLUSIONS

In summary, (18-crown-6)stilbene (*E*)-**S** can bind the ethanediammonium ion $\mathbf{A}^{2+}$ in MeCN to form 1:1 and 2:2 (stilbene-to-dication) complexes, the latter having a pseudo-sandwich structure. UV irradiation of a 2:1 mixture of (*E*)-**S** and $\mathbf{A}^{2+}$ gives mainly cyclobutane *rctt*-**C** and phenanthrene **P**. The fact that the PCA reaction of stilbene (*E*)-**S** occurs selectively to produce the single cyclobutane isomer *rctt*-**C** is explained by the supramolecular pre-organization of stilbene molecules into a pseudo-sandwich complex $[(E)\text{-}\mathbf{S}]_2{\cdot}\mathbf{A}^{2+}$. Cycloadduct *rctt*-**C** was isolated by preparative photolysis, followed by chromatography. In comparison with the previously studied complex $(\mathbf{BCS})_2{\cdot}(\mathbf{A}^{2+})_2$ formed due to two-site coordination, the $[(E)\text{-}\mathbf{S}]_2{\cdot}\mathbf{A}^{2+}$ complex (one-site

https://doi.org/10.1021/acsomega.2c05295
ACS Omega 2022, 7, 42370−42376

coordination) is characterized by a much lower PCA quantum yield. This is caused by a small population of stacked conformers in the case of $[(E)\text{-}\mathbf{S}]_2\cdot\mathbf{A}^{2+}$ as well as by less favorable arrangement of the olefinic bonds for the PCA reaction. The results of this study extend the scope of applicability of PCA reactions by the use of monocrown diarylethylenes and supramolecular organization. They may be useful for developing synthetic routes to macrocyclic cyclobutane derivatives, which are of interest as new types of photoswitchable host molecules. It was also shown that while considering the photochemistry of dimeric structures of aromatic olefins, one should take into account the possibility of photoinduced electrocyclic reactions.

EXPERIMENTAL SECTION

General. ^{1}H NMR spectra were recorded on a Bruker AVANCE III 500 MHz BioSpin (500.20 MHz) instrument in DMSO-d_6 or MeCN-d_3 using the solvent as the internal standard (δ_H 2.50 and 1.94 ppm, respectively). Electrospray ionization (ESI) mass spectra were acquired using an Exactive Orbitrap mass spectrometer (ThermoFisher Scientific, Germany) and a home-made electrospray ion source. The working resolution of the mass spectrometer in the reported experiments was 10000 (FWHM), the accuracy of m/z measurements was better than 5 ppm, and the mass spectrum registration time was 1 min. The electrospray ion source characteristics were as follows: quartz capillary inner diameter of 50 μm, capillary high voltage of $\pm$3 kV, and sample solution flow rate of 1.0 μL/min. Electronic absorption spectra were recorded on a Specord 250 Plus spectrophotometer in quartz cells with ground-in stoppers. All manipulations with solutions of compound **S** were performed in a darkroom under red light (daylight induces the $E-Z$ photoisomerization). Steady-state photolysis was carried out using glass-filtered light (λ = 313 nm) of a DRSh-250 high-pressure mercury lamp (250 W). The 313 nm spectral line was isolated with an efficiency of 99.0% using a combination of optical filters UFS-2 (3 mm thick) and ZhS-3 (2.5 mm thick). Low-pressure mercury lamp (4 W) with an appropriate light filter was used as a light source with λ = 254 nm. The intensity of actinic light was measured by chemical actinometry. Isolation of cyclobutane derivative *rctt*-**C** was done by TLC on DC-Alufolien Aluminiumoxid 60 F_{254} neutral (Typ E) (Merck). Chloroform was chemical pure (99%). MeCN (special purity grade, water content <0.03%, v/v, Cryochrom) was used to prepare the solutions. Ethane-1,2-diammonium diperchlorate $\mathbf{A}(ClO_4)_2$ was obtained according to the known procedure.[27]

18,18′-((1*R*,2*S*,3*R*,4*S*)-3,4-Diphenylcyclobutane-1,2-diyl)bis(2,3,5,6,8,9,11,12,14,15-decahydrobenzo[*b*][1,4,7,10,13,16]hexaoxacyclooctadecine) (*rctt*-C). A mixture of crown stilbene (E)-**S** (20.4 mg, 49.2 μmol) and ethanediammonium diperchlorate $\mathbf{A}(ClO_4)_2$ (6.83 mg, 26.2 μmol) in MeCN (12 mL) was saturated with argon for 15 min. Then, the solution was irradiated at 313 nm for 80 h. The photolysate was concentrated to 2 mL, and then water (18 mL) was added. The resulting mixture was extracted with chloroform. The extracts (3 × 15 mL) were combined and evaporated to dryness in air at room temperature. The residue was dissolved in a minor amount of MeCN, separated in a thin film on a neutral Al_2O_3 plate, and eluted with a $CHCl_3$/MeCN mixture with a gradual increase in the MeCN fraction to 50%. The major (dark at 254 nm light) fraction was collected. Alumina was transferred on a glass filter and washed with pure MeCN (10 ml). The solution was evaporated to dryness in air for 2 days. This gave ∼2 mg (∼5%) of a white powder. ^{1}H NMR (500 MHz, MeCN-d_3): δ (ppm) 7.21−7.16 (m, 2H), 7.13 (t, 2H, J = 7.6 Hz), 7.04 (t, 1H, J = 7.3 Hz), 6.78 (dd, 1H, J = 8.3, 2.0 Hz), 6.78 (d, 1H, J = 8.2 Hz), 6.68 (d, 1H, J = 8.2 Hz), 4.47 (d, 1H, J = 7.2 Hz), 4.39 (d, 1H, J = 7.2 Hz), 4.04−3.99 (m, 2H), 3.99−3.93 (m, 2H), 3.75−3.69 (m, 2H), 3.69−3.63 (m, 2H), 3.62−3.48 (m, 14H). HRMS-ESI: calcd for $C_{48}H_{60}NaO_{12}^+$ $[M + Na]^+$ 851.3977; found, 851.4030.

Spectrophotometric Titration (SPT). Titration experiments were conducted in MeCN in 0.2 and 4.75 cm cells. In the (E)-**S**−$\mathbf{A}(ClO_4)_2$ system, the total concentration of stilbene (E)-**S** was maintained, and the total concentration of the salt $\mathbf{A}(ClO_4)_2$ increased incrementally starting from zero. The stability constants and the absorption spectra of pure complexes $[(E)\text{-}\mathbf{S}]_2\cdot\mathbf{A}^{2+}$ and $(E)\text{-}\mathbf{S}\cdot\mathbf{A}^{2+}$ were determined by globally fitting the SPT data to a definite complexation model[22]

$$S + A \overset{K_{1:1}}{\rightleftharpoons} S\cdot A^{2+} \quad (1)$$

$$S\cdot A^{2+} + S \overset{K_{2:1}}{\rightleftharpoons} S_2\cdot A^{2+} \quad (2)$$

where S and A^{2+} are the stilbene molecule (E)-**S** and alkanediammonium dication $\mathbf{A}^{2+}$, respectively, $S\cdot A^{2+}$ is their 1:1 complex, $S_2\cdot A^{2+}$ is the pseudo-sandwich 2:1 complex, and $K_{1:1}$ and $K_{2:1}$ are the stability constants of $S\cdot A^{2+}$ and $S_2\cdot A^{2+}$, respectively. The calculation took into account the results of two SPTs carried out in different cells and with two different absolute concentrations of the ligand (Figures S8 and S9).

^{1}H NMR TITRATION

The experiment was conducted in MeCN-d_3 in a 5 mm NMR tube (Norell). The chemical shifts were estimated by approximation of the multiplets by a sum of Lorentzian functions after baseline correction using polynomials of different orders. The dependences of chemical shifts δ on the concentration C_A at a constant concentration C_S for various protons were adequately approximated by global analysis[22] using two equilibria (1 and 2) under the following assumption

$$\delta = ([S]\delta_S + [S\cdot A^{2+}]\delta_{1:1} + 2[S_2\cdot A^{2+}]\delta_{2:1})/C_S \quad (3)$$

where δ_S, $\delta_{1:1}$, and $\delta_{2:1}$ are the chemical shits of S, $S\cdot A^{2+}$, and $S_2\cdot A^{2+}$ signals, respectively.

PCA QUANTUM YIELDS

A mixture of the stilbene (E)-**S** (1×10^{-4} M) and $\mathbf{A}(ClO_4)_2$ (5×10^{-5} M) in MeCN (0.2 cm cell) was steady-state irradiated at 313 nm. The total effective quantum yield Φ_{tot} of the stilbene **S** consumption was derived from the kinetics of the absorption spectra using the kinetic equation for irreversible unimolecular photoreactions

$$\frac{dC_S(t)}{dt} = -\Phi_{tot} I 10^3 \frac{(1 - 10^{-D_{tot}})}{l}\frac{D_S}{D_{tot}} \quad (4)$$

$$D_S = \varepsilon_{EZ} C_S l,\ D_{tot} = \varepsilon_{EZ} C_S l + \varepsilon_P C_P l$$

where C_S is the overall concentration of the E- and Z-isomers of stilbene **S**, mol L^{-1}; I is the actinic light intensity, mol·$cm^{-2}s^{-1}$; l is the cell length, cm; ε_{EZ} is the molar absorptivity of the $E-Z$ photostationary mixture at the irradiation wavelength, L $mol^{-1}cm^{-1}$; ε_P is the molar absorptivity of the photolysate at

https://doi.org/10.1021/acsomega.2c05295
ACS Omega 2022, 7, 42370−42376

the irradiation wavelength, L $mol^{-1}cm^{-1}$; and C_P is the concentration of the photolysate, mol L^{-1}. The quasi–photostationary equilibrium between the *E*- and *Z*-isomers of stilbene **S**, rapidly attained due to efficient photoisomerization, was taken as the starting point (the red curve in Figure 4, the black curve in Figure S22a). The Φ_{tot} value (0.0011) was determined from the initial segment of the kinetic curve. Then, Φ_{tot} was multiplied by the fraction of cyclobutane *rctt*-**C** (0.50) in the photolysate mixture, thus giving Φ_{PCA} (Figure S15). The considered photolysis products included cyclobutane *rctt*-**C**, phenanthrene **P**, benzaldehyde, and 4′-formylbenzo-18-crown-6 ether (**F**). In the case of determination of Φ_{EL}, the Φ_{tot} value was multiplied by the fraction of phenanthrene **P** (0.37) in the photolysate (Figure S15). The measured quantum yields are effective values because we did not take into account the partial concentration of the $[(E)\text{-}\mathbf{S}]_2{\cdot}\mathbf{A}^{2+}$ complex in solution and the contribution of its optical density to the observed optical density.

Density Functional Theory (DFT) Calculations. DFT calculations were performed using the Gaussian 09 program package.[28] Geometry optimizations were carried out with the M06-2X functional[29] and the 6-31G(d) basis set. The default optimization criteria were tightened three times using the internal option IOp(1/7 = 100). The SMD polarizable continuum model[30] was employed to simulate the effects of MeCN as the experimental solvent. All geometry optimizations were followed by frequency calculations to verify the nature of stationary points and to compute the thermochemical quantities. The thermochemical analysis was carried out using a scale factor of 0.9678 for harmonic frequencies.[31] The Gibbs free energy in solution (G_{soln}) was calculated by the formula

$$G_{soln} = E_{soln} + \Delta G_{corr} \quad (5)$$

where E_{soln} is the electronic energy in solution and ΔG_{corr} is the thermal correction to the free energy, including the zero-point vibrational energy.

■ ASSOCIATED CONTENT

Supporting Information

The Supporting Information is available free of charge at https://pubs.acs.org/doi/10.1021/acsomega.2c05295.

NMR and mass spectra, spectrophotometric and NMR titrations data, and details of the DFT calculations (PDF)

■ AUTHOR INFORMATION

Corresponding Authors

Timofey P. Martyanov − *Federal Research Center of Problems of Chemical Physics and Medicinal Chemistry, Russian Academy of Sciences, Moscow Region 142432, Russian Federation; Photochemistry Center of RAS, FSRC "Crystallography and Photonics", Russian Academy of Sciences, Moscow 119421, Russian Federation;* orcid.org/0000-0002-1537-9776; Email: martyanov.t@gmail.com

Sergey P. Gromov − *Photochemistry Center of RAS, FSRC "Crystallography and Photonics", Russian Academy of Sciences, Moscow 119421, Russian Federation; Department of Chemistry, Lomonosov Moscow State University, Moscow 119991, Russian Federation;* orcid.org/0000-0002-2542-7807; Email: spgromov@mail.ru

Authors

Artem P. Vorozhtsov − *Federal Research Center of Problems of Chemical Physics and Medicinal Chemistry, Russian Academy of Sciences, Moscow Region 142432, Russian Federation; Photochemistry Center of RAS, FSRC "Crystallography and Photonics", Russian Academy of Sciences, Moscow 119421, Russian Federation*

Nadezhda A. Aleksandrova − *Photochemistry Center of RAS, FSRC "Crystallography and Photonics", Russian Academy of Sciences, Moscow 119421, Russian Federation*

Ilia V. Sulimenkov − *Chernogolovka Branch of the N.N. Semenov Federal Research Center for Chemical Physics, Russian Academy of Sciences, Moscow Region 142432, Russian Federation*

Evgeny N. Ushakov − *Federal Research Center of Problems of Chemical Physics and Medicinal Chemistry, Russian Academy of Sciences, Moscow Region 142432, Russian Federation; Photochemistry Center of RAS, FSRC "Crystallography and Photonics", Russian Academy of Sciences, Moscow 119421, Russian Federation;* orcid.org/0000-0002-9969-5185

Complete contact information is available at: https://pubs.acs.org/10.1021/acsomega.2c05295

Notes

The authors declare no competing financial interest.

■ ACKNOWLEDGMENTS

This work was supported by the Russian Science Foundation (project no. 22-13-00064, except NMR titration and mass spectrometry). The mass spectrometry analysis and NMR titration were done under financial support of the Ministry of Science and Higher Education of the Russian Federation (State Assignments no. 122040500059-8 and no. AAAA-A19-119070790003-7, respectively).

■ REFERENCES

(1) Hoffmann, N. Photochemical Reactions as Key Steps in Organic Synthesis. *Chem. Rev.* **2008**, *108*, 1052−1103.

(2) Bach, T.; Hehn, J. P. Photochemical Reactions as Key Steps in Natural Product Synthesis. *Angew. Chem., Int. Ed.* **2011**, *50*, 1000−1045.

(3) Poplata, S.; Tröster, A.; Zou, Y.-Q.; Bach, T. Recent Advances in the Synthesis of Cyclobutanes by Olefin [2 + 2] Photocycloaddition Reactions. *Chem. Rev.* **2016**, *116*, 9748−9815.

(4) Urriolabeitia, E. P.; Sánchez, P.; Pop, A.; Silvestru, C.; Laga, E.; Jiménez, A. I.; Cativiela, C. Synthesis of esters of diaminotruxillic bis-amino acids by Pd-mediated photocycloaddition of analogs of the Kaede protein chromophore. *Beilstein J. Org. Chem.* **2020**, *16*, 1111−1123.

(5) Triandafillidi, I.; Nikitas, N. F.; Gkizis, P. L.; Spiliopoulou, N.; Kokotos, C. G. Hexafluoroisopropanol-Promoted or Brønsted Acid-Mediated Photochemical [2+2] Cycloadditions of Alkynes with Maleimides. *ChemSusChem* **2022**, *15*, No. e202102441.

(6) Chung, C.-M.; Roh, Y.-S.; Cho, S.-Y.; Kim, J.-G. Crack Healing in Polymeric Materials via Photochemical [2+2] Cycloaddition. *Chem. Mater.* **2004**, *16*, 3982−3984.

(7) Wang, Y.; Liu, Q.; Li, J.; Ling, L.; Zhang, G.; Sun, R.; Wong, C.-P. UV-triggered self-healing polyurethane with enhanced stretchability and elasticity. *Polymer* **2019**, *172*, 187−195.

(8) Ushakov, E. N.; Gromov, S. P. Supramolecular methods for controlling intermolecular [2+2] photocycloaddition reactions of unsaturated compounds in solutions. *Russ. Chem. Rev.* **2015**, *84*, 787−802.

(9) Ramamurthy, V.; Sivaguru, J. Supramolecular Photochemistry as a Potential Synthetic Tool: Photocycloaddition. *Chem. Rev.* **2016**, *116*, 9914−9993.
(10) Bibal, B.; Mongin, C.; Bassani, D. M. Template effects and supramolecular control of photoreactions in solution. *Chem. Soc. Rev.* **2014**, *43*, 4179−4198.
(11) Berdnikova, D. V.; Aliyeu, T. M.; Delbaere, S.; Fedorov, Yu. V.; Jonusauskas, G.; Novikov, V. V.; Pavlov, A. A.; Peregudov, A. S.; Shepel', N. E.; Zubkov, F. I.; Fedorova, O. A. Regio- and stereoselective [2+2] photocycloaddition in Ba^{2+} templated supramolecular dimers of styryl-derivatized aza-heterocycles. *Dyes Pigm.* **2017**, *139*, 397−402.
(12) Pattabiraman, M.; Sivaguru, J.; Ramamurthy, V. Cucurbiturils as Reaction Containers for Photocycloaddition of Olefins. *Isr. J. Chem.* **2018**, *58*, 264−275.
(13) Jon, S. Y.; Ko, Y. H.; Park, S. H.; Kim, H.-J.; Kim, K. A facile, stereoselective [2 + 2] photoreaction mediated by cucurbit[8]uril. *Chem. Commun.* **2001**, 1938−1939.
(14) Pattabiraman, M.; Natarajan, A.; Kaliappan, R.; Mague, J. T.; Ramamurthy, V. Template directed photodimerization of *trans*-1,2-bis(*n*-pyridyl)ethylenes and stilbazoles in water. *Chem. Commun.* **2005**, 4542−4544.
(15) Ananchenko, G. S.; Udachin, K. A.; Ripmeester, J. A.; Perrier, T.; Coleman, A. W. Phototransformation of stilbene in van der Waals nanocapsules. *Chem. Eur. J.* **2006**, *12*, 2441−2447.
(16) Gromov, S. P.; Vedernikov, A. I.; Sazonov, S. K.; Kuz'mina, L. G.; Lobova, N. A.; Strelenko, Yu. A.; Howard, J. A. K. Synthesis, structure, and stereospecific cross-[2+2] photocycloaddition of pseudodimeric complexes based on ammonioalkyl derivatives of styryl dyes. *New J. Chem.* **2016**, *40*, 7542−7556.
(17) Martyanov, T. P.; Vedernikov, A. I.; Ushakov, E. N.; Sazonov, S. K.; Aleksandrova, N. A.; Lobova, N. A.; Kuz'mina, L. G.; Howard, J. A. K.; Alfimov, M. V.; Gromov, S. P. Pseudodimeric complexes of 4-styrylpyridine derivatives: Structure−property relationships and a stereospecific [2+2]-cross-photocycloaddition in solution. *Dyes Pigm.* **2020**, *172*, 107825.
(18) Martyanov, T. P.; Ushakov, E. N.; Nuriev, V. N.; Aleksandrova, N. A.; Sazonov, S. K.; Vedernikov, A. I.; Kuz'mina, L. G.; Klimenko, L. S.; Martyanova, E. G.; Gromov, S. P. Pseudodimeric Complexes of an (18-Crown-6)stilbene with Styryl Dyes Containing an Ammonioalkyl Group: Synthesis, Structure, and Stereospecific [2 + 2] Cross-Photocycloaddition. *J. Org. Chem.* **2021**, *86*, 3164−3175.
(19) Gromov, S. P.; Vedernikov, A. I.; Kuz'mina, L. G.; Lobova, N. A.; Basok, S. S.; Strelenko, Yu. A.; Alfimov, M. V. Stereoselective [2+2] photocycloaddition in bispseudosandwich complexes of bis(18-crown-6) stilbene with alkanediammonium ions. *Russ. Chem. Bull.* **2009**, *58*, 108−114.
(20) Gromov, S. P.; Vedernikov, A. I.; Lobova, N. A.; Kuz'mina, L. G.; Basok, S. S.; Strelenko, Y. A.; Alfimov, M. V.; Howard, J. A. K. Controlled self-assembly of bis(crown)stilbenes into unusual bis-sandwich complexes: structure and stereoselective [2+2] photocycloaddition. *New J. Chem.* **2011**, *35*, 724−737.
(21) Ushakov, E. N.; Martyanov, T. P.; Vedernikov, A. I.; Pikalov, O. V.; Efremova, A. A.; Kuz'mina, L. G.; Howard, J. A. K.; Alfimov, M. V.; Gromov, S. P. Self-assembly through hydrogen bonding and photochemical properties of supramolecular complexes of bis(18-crown-6)stilbene with alkanediammonium ions. *J. Photochem. Photobiol. A: Chem.* **2017**, *340*, 80−87.
(22) Ushakov, E. N.; Gromov, S. P.; Fedorova, O. A.; Pershina, Yu. V.; Alfimov, M. V.; Barigelletti, F.; Flamigni, L.; Balzani, V. Sandwich-Type Complexes of Alkaline-Earth Metal Cations with a Bisstyryl Dye Containing Two Crown Ether Units. *J. Phys. Chem. A* **1999**, *103*, 11188−11193.
(23) Rafiq, S. M.; Sivasakthikumaran, R.; Mohanakrishnan, A. K. Lewis Acid/Brönsted Acid Mediated Benz-Annulation of Thiophenes and Electron-Rich Arenes. *Org. Lett.* **2014**, *16*, 2720−2723.
(24) Doany, F. E.; Hochstrasser, R. M.; Greene, B. I.; Millard, R. R. Femtosecond-resolved ground-state recovery of cis-stilbene in solution. *Chem. Phys. Lett.* **1985**, *118*, 1−5.
(25) Ramamurthy, V.; Venkatesan, K. Photochemical Reactions of Organic Crystals. *Chem. Rev.* **1987**, *87*, 433−481.
(26) Wheeler, S. E. Understanding Substituent Effects in Noncovalent Interactions Involving Aromatic Rings. *Acc. Chem. Res.* **2013**, *46*, 1029−1038.
(27) Vedernikov, A. I.; Ushakov, E. N.; Lobova, N. A.; Kiselev, A. A.; Alfimov, M. V.; Gromov, S. P. Photosensitive molecular tweezers. 3. Synthesis and homoditopic complex formation of a bisstyryl dye containing two crown-ether fragments with diammonium salts. *Russ. Chem. Bull.* **2005**, *54*, 666−672.
(28) Frisch, M. J.; Trucks, G. W.; Schlegel, H. B.; Scuseria, G. E.; Robb, M. A.; Cheeseman, J. R.; Scalmani, G.; Barone, V.; Mennucci, B.; Petersson, G. A.; Nakatsuji, H.; Caricato, M.; Li, X.; Hratchian, H. P.; Izmaylov, A. F.; Bloino, J.; Zheng, G.; Sonnenberg, J. L.; Hada, M.; Ehara, M.; Toyota, K.; Fukuda, R.; Hasegawa, J.; Ishida, M.; Nakajima, T.; Honda, Y.; Kitao, O.; Nakai, H.; Vreven, T.; Montgomery, J. A.; Peralta, J. E., Jr.; Ogliaro, F.; Bearpark, M.; Heyd, J. J.; Brothers, E.; Kudin, K. N.; Staroverov, V. N.; Kobayashi, R.; Normand, J.; Raghavachari, K.; Rendell, A.; Burant, J. C.; Iyengar, S. S.; Tomasi, J.; Cossi, M.; Rega, N.; Millam, J. M.; Klene, M.; Knox, J. E.; Cross, J. B.; Bakken, V.; Adamo, C.; Jaramillo, J.; Gomperts, R.; Stratmann, R. E.; Yazyev, O.; Austin, A. J.; Cammi, R.; Pomelli, C.; Ochterski, J. W.; Martin, R. L.; Morokuma, K.; Zakrzewski, V. G.; Voth, G. A.; Salvador, P.; Dannenberg, J. J.; Dapprich, S.; Daniels, A. D.; Farkas, Ö.; Foresman, J. B.; Ortiz, J. V.; Cioslowski, J.; Fox, D. J.*Gaussian 09, Revision 01*; Gaussian, Inc.: Wallingford CT, 2013.
(29) Zhao, Y.; Truhlar, D. G. The M06 Suite of Density Functionals for Main Group Thermochemistry, Thermochemical Kinetics, Noncovalent Interactions, Excited States, and Transition Elements: Two New Functionals and Systematic Testing of Four M06-Class Functionals and 12 Other Functionals. *Theor. Chem. Acc.* **2008**, *120*, 215−241.
(30) Marenich, A. V.; Cramer, C. J.; Truhlar, D. G. Universal Solvation Model Based on Solute Electron Density and on a Continuum Model of the Solvent Defined by the Bulk Dielectric Constant and Atomic Surface Tensions. *J. Phys. Chem. B* **2009**, *113*, 6378−6396.
(31) Kesharwani, M. K.; Brauer, B.; Martin, J. M. L. Frequency and Zero-Point Vibrational Energy Scale Factors for Double-Hybrid Density Functionals (and Other Selected Methods): Can Anharmonic Force Fields Be Avoided? *J. Phys. Chem. A* **2015**, *119*, 1701−1714.

https://doi.org/10.1021/acsomega.2c05295
ACS Omega 2022, 7, 42370−42376